Observation of Ferromagnetic and Antiferromagnetic Coupling in 1-D and 2-D Extended Structures of Copper(II) Terephthalates

Laura Deakin, Atta M. Arif, and Joel S. Miller*

Department of Chemistry, University of Utah, 315 South 1400 East Rm. Dock, Salt Lake City, Utah 84112-0850

Received April 12, 1999

The reaction between $CuCl_2 \cdot 2H_2O$ and disodium terephthalate, Na_2**tp**, in aqueous solution simultaneously produces chain, bis(aqua)[μ-(terephthalato-κO:κO′)]copper(II), monohydrate, Cu**tp**$(OH_2)_2 \cdot H_2O$ (**1**), and layered, bis(aqua)-[μ-(terephthalato-κO)]copper(II), Cu**tp**$(OH_2)_2$ (**2**), structured materials. **1** ($C_8H_{10}CuO_7$) belongs to the orthorhombic $P2_12_12$ space group [$a = 6.3015(4)$ Å, $b = 6.8743(4)$ Å, $c = 22.9972(14)$ Å, and $Z = 4$] and incorporates **tp** in a bridging bis-monodentate binding mode and Cu(II) in a tetragonally elongated octahedron. **2** ($C_8H_{10}CuO_6$) which belongs to the orthorhombic $Pmc2_1$ space group [$a = 10.7421(8)$ Å, $b = 7.2339(10)$ Å, $c = 5.7143(13)$ Å, and $Z = 2$] incorporates **tp** in a mono-bidentate binding mode and Cu(II) in a distorted square pyramid. **1** and **2** exhibit axial X-band powder EPR spectra with $g_\perp = 2.08$, $g_\parallel = 2.29$ (**1**) and $g_\perp = 2.07$, $g_\parallel = 2.29$ (**2**) at 300 K. **1** obeys the Curie−Weiss law at high temperatures ($\theta = -7.2$ K) and at low temperatures behaves as 1-D magnetic chains with an exchange-coupling constant of $J/k_B = -9.15$ K ($H = -2J\mathbf{S}_1 \cdot \mathbf{S}_2$). This material displays a spontaneous moment below 2 K under small applied magnetic fields, consistent with the presence of spin canting. **2** exhibits ferromagnetic interactions with $\theta = +0.8$ K. Along the 1-D chain where coordinated water forms the bridge between metal centers, the coupling between Cu(II) is $J/k_B = +0.6$ K. The fit of the magnetic susceptibility for **2** using a molecular field correction, which takes into consideration antiferromagnetic interactions between chains via the **tp** ligand, yields $J'/k_B = -0.13$ K.

Introduction

The recent work dedicated to the study of molecular-based magnets is driven in part by the need to understand the fundamental science associated with magnetic interactions observed between organic or inorganic spin carriers and develop structure−function relationships enabling the design synthesis of new magnetic materials.[1] This field within materials chemistry encompasses the development of magnetically interesting systems coupled to the so-called crystal "engineering" approach extensively used to control material structure and dimensionality in which inorganic extended structures with organic bridges are produced based on coordination polymers or networks.[2] These magnetic systems can be constructed to yield 1-, 2-, or 3-D extended structures, with the metal center being the lone carrier of unpaired spin, and the diamagnetic bridging ligands provide a superexchange pathway which determines the strength and type of magnetic coupling, *J*.

Herein, the magnetic properties of extended structures, two pseudopolymorphs formed upon binding terephthalate (1,4-benzenedicarboxylate ≡ **tp**) to Cu(II) metal centers and differing by one water, are examined. This reaction of $Cu^{II}_2(acetate)_4$ and $[piperdinium]_2$**tp** has been reported to form an amorphous precipitate of unknown structure which magnetically orders at 13 K.[3] As the structure of the product of this reaction could not be determined, the Cu−**tp** bonding in this material that leads to this unexpectedly high ordering temperature could not be addressed. It should be noted that this is the highest reported ordering temperature for a material obtained from the reaction of Cu(II) with **tp**. To further understand the magnetic properties associated with different binding modes of **tp** with Cu(II), we have synthesized extended structures based upon **tp**-bridged Cu-(II) metal centers.

The use of dicarboxylic acids to form bridges between paramagnetic metal centers has been extensively studied, with the majority of materials being oxalato-bridged Cu(II) centers, displaying both strongly and weakly antiferromagnetically coupled metal centers.[4] Benzoic acid-based ligands have led to a variety of structures as these ligands can form short bridges

(1) Reviews: (a) Miller, J. S.; Epstein, A. J. *Angew. Chem., Int. Ed. Engl.* **1994**, *33*, 385. (b) Miller, J. S.; Epstein, A. J. *Adv. Chem. Ser.* **1995**, *245*, 161. (c) Buchachenko, A. L. *Russ. Chem. Rev.* **1990**, *59*, 307. (d) Kahn, O. *Struct. Bonding* **1987**, *68*, 89. (e) Caneschi, A.; Gatteschi, D.; Sessoli, R.; Rey, P. *Acc. Chem. Res.* **1989**, *22*, 392. (f) Gatteschi, D. *Adv. Mater.* **1994**, *6*, 635. (g) Miller, J. S.; Epstein, A. J.; Reiff, W. M. *Acc. Chem. Res.* **1988**, *21*, 114. (h) Miller, J. S.; Epstein, A. J.; Reiff, W. M. *Science* **1988**, *240*, 40. (i) Miller, J. S.; Epstein, A. J.; Reiff, W. M. *Chem. Rev.* **1988**, *88*, 201. (j) Miller, J. S.; Epstein, A. J. In *New Aspects of Organic Chemistry;* Yoshida, Z., Shiba, T., Oshiro, Y., Eds.; VCH Publishers: New York, 1989; Vol. 237. (k) Miller, J. S.; Epstein, A. J. *Chem. Eng. News* **1995**, *73* (40), 30. (l) Kahn, O. *Molecular Magnetism*; VCH Publishers: New York, 1993.

(2) (a) Coronado, E.; Delhaès, P.; Gatteschi, D.; Miller, J. S. *Molecular Magnetism: From Molecular Assemblies to the Devices*; Kluwer Academic Publishers: Dordrecht, The Netherlands, 1996. (b) Robson, R.; Abrahams, G. F.; Batten, S. R.; Gable, R. W.; Hoskins, B. F.; Liu, J. *Supramolecular Architecture*; American Chemical Society: Washington, DC, 1992. (c) Subramanian, S.; Zaworotko, M. J. *Angew. Chem., Int. Ed. Engl.* **1995**, *34*, 2127. (d) Chen, C. T.; Suslick, K. *Coord. Chem. Rev.* **1993**, *128*, 293.

(3) Bakalbassis, E.; Kahn, O.; Bergerat, P.; Jeannin, S.; Jeannin, Y.; Dromzee, Y. *J. Chem. Soc., Chem. Commun.* **1990**, 1771.

(4) (a) DeMunno, G.; Lloret, F.; Julve, M. In *Magnetism: A Supramolecular Function*; Kahn, O., Ed.; Kluwer Academic Publishers: Dordrecht, The Netherlands, 1996; p 555. (b) Michalowicz, A.; Girerd, J. J.; Goulon, J. *Inorg. Chem.* **1979**, *18*, 3004. (c) Girerd, J. J.; Kahn, O.; Verdaguer, M. *Inorg. Chem.* **1980**, *19*, 274. (d) Akhriff, Y.; Server-Carrio, J.; Sancho, A.; Garcia-Lozano, J.; Escriva, E.; Folgado, J. V.; Soto, L. *Inorg. Chem.* **1999**, *38*, 1174.

10.1021/ic990400r CCC: $18.00
Published on Web 10/02/1999

via one carboxolato end, or longer bridges through the benzene ring. Recent reports of **tp**-bridged Cu(II) centers have included the ligand as being coordinated to the metal in either a chelating bis-bidentate[5] (**A**) or bis-monodentate (**B**)[5−8] or bridging bis-monodentate (syn−syn) (**C**)[9] fashion. Materials containing both

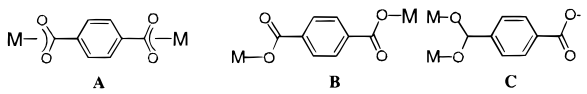

short and long bridges have been reported with **tp**-bridged Mn(II)[10] and Cu(II) complexes.[9] Long **tp** bridges typically produce M···M separations of ∼11 Å, which generally leads to weak antiferromagnetic interactions between metal centers, $J/k_B \leq -2$ K for M = Mn, Co, Ni, and Cu,[5] where $H = -2J\sum \mathbf{S}_1 \cdot \mathbf{S}_2$. When both the metal basal planes and the ligand are coplanar, a much stronger antiferromagnetic interaction is observed ($J \approx -100$ K);[6] however, the loss of coordinated water molecules leading to the formation of **tp** bridges, during magnetic measurements, may account for such large interactions.[5a]

This is in contrast to the very strongly antiferromagnetically coupled short carboxylato-bridged $Cu^{II}_2(O_2CR)_4$ (R = $-CMe_3$,[11] $-C{\equiv}CPh$,[12] $-C(O)Ph$[13]) dimers that display coupling of $J/k_B \approx -215$, -230, and -940 K, respectively. For these systems, the degree of the magnetic interaction in Cu(II) dimers has been correlated to the pK_a of the parent carboxylic acid for a variety of bridging ligands.[14]

Experimental Section

Synthesis. Disodium terephthalate was produced from the reaction between terephthalic acid (ACROS, 6.61 mol) and NaOH (ACROS, 13.45 mol) in distilled water. Crystals were grown by slow diffusion over several days by placing sodium terephthalate (0.0735 mmol) and $CuCl_2 \cdot 2H_2O$ (0.075 mmol) in distilled water (10 mL) in an "H"-tube. Single crystals of light blue blocks (**1**) of Cu**tp**$(OH_2)_2 \cdot H_2O$ composition and dark blue prisms (**2**) of Cu**tp**$(OH_2)_2$ composition were obtained after several days, and separated manually. (**1**) IR (KBr): 1544(s), 1502(s), 1428(s), 1393(s), 1294(m) cm^{-1}; EPR (300 K): $g_\perp = 2.08$, $g_\parallel = 2.29$. TGA: 15% weight loss between 80 and 120 °C. (**2**) IR (KBr): 1691(m), 1579(s), 1510(s), 1397(s), 1299(m) cm^{-1}; EPR (300 K): $g_\perp = 2.07$, $g_\parallel = 2.29$. TGA: 12% weight loss between 120 and 220 °C.

Physical Measurements. Infrared spectra were taken on a Bio-Rad FTS-40 spectrophotometer (±2 cm^{-1}) as KBr pellets. The thermal properties were studied on a TA Instruments Model 2050 thermogravimetric analyzer (TGA) equipped with an electron spray mass spectrometer, located in a Vacuum Atmospheres DriLab under argon. Samples were heated between room temperature and 450 °C at 20 °C/min. Magnetic measurements for powder samples were acquired on a Quantum Design MPMS-5XL SQUID magnetometer as previously described[15] and were corrected for the diamagnetism of the sample (-120×10^{-6} emu/mol) and the sample holder, and for the temperature-independent paramagnetism of Cu(II) of 60×10^{-6} emu/mol. Samples were cooled under zero field to 2 K, and then warmed under an applied field. Powder EPR spectra were recorded using a Bruker EMX X-band spectrometer with 1,1-diphenyl-2-picrylhydrazyl (Sigma) as an external standard ($g = 2.0037$[16]).

Table 1. Crystallographic Data Collection and Structure Refinement Parameters for Cu**tp**$(OH_2)_2 \cdot H_2O$ (**1**), and Cu**tp**$(OH_2)_2$ (**2**)

	Cu**tp**$(OH_2)_2 \cdot H_2O$ (**1**)	Cu**tp**$(OH_2)_2$ (**2**)
empirical formula	$C_8H_8CuO_6$	$C_8H_{10}CuO_7$
formula mass, Da	281.70	263.68
space group	$P2_12_12$	$Pmc2_1$
a = Å	6.3015(4)	10.7421(8)
b = Å	6.8743(4)	7.2339(10)
c = Å	22.9972(14)	5.7143(13)
V, Å^3	996.20(11)	444.04(12)
ρ_{calcd}, cm^{-3}	1.878	1.872
T, °C	27	−112
λ, Å	0.710 73	0.710 73
R1(F_o^2)[a]	0.0268	0.0418
wR2(F_o^2)[b]	0.0772	0.1057
Z	4	2
μ, mm^{-1}	2.211	2.465

[a] $R1 = \sum(||F_o| - |F_c||)/\sum|F_o|$. [b] $wR2 = [\sum(w(F_o^2 - F_c^2)^2)/\sum(F_o^2)^2]^{1/2}$.

Single-Crystal X-ray Structure Determination. Diffraction measurements were made on a Nonius KappaCCD diffractometer equipped with Mo Kα radiation. Indexing and unit cell refinement were based on all observed reflections from 10 frames collected at 200 K with an oscillation range of 1 deg/frame and an exposure time of 30 s/frame. The details of the diffraction studies are summarized in Table 1. The structures of **1** and **2** were solved by direct methods using the program SIR-97[17] and were refined by a full-matrix least-squares method on F^2 with SHELXL 97.[18] Anisotropic thermal parameters were assigned to Cu, C, and O atoms, while hydrogen atoms were located by difference maps and their positions isotropically refined. Scattering factors were taken from the *International Tables for Crystallography*.[19] ORTEP diagrams were generated using ORTEP 3.[20]

Results and Discussion

The aqueous reaction of Na_2**tp** and $CuCl_2 \cdot 2H_2O$ leads to the isolation of bis(aqua)[μ-(terephthalato-κO:κO′)]copper(II) monohydrate, Cu**tp**$(OH_2)_2 \cdot H_2O$ (**1**), and bis(aqua)[μ-(terephthalato-κO)]Copper(II), Cu**tp**$(OH_2)_2$ (**2**). These pseudopolymorphs exhibit different extended structures and different magnetic properties. There are only a few reports of **tp**-bridged Cu(II) centers that lead to extended structures. The reaction between Cu(II) and terephthalate in the presence of coordinating amines has led to the characterization of chain[8] and sheet[9] structures. Interestingly, the latter are reported to display strong antifer-

(5) (a) Cano, J.; DeMunno, G.; Sanz, J. L.; Ruiz, R.; Faus, J.; Lloret, F.; Julve, M.; Caneschi, A. *J. Chem. Soc., Dalton Trans*. **1997**, 1915. (b) Bakalbassis, E. G.; Mrozinski, J.; Tsipis, C. A. *Inorg. Chem*. **1986**, *25*, 3684. (c) Verdaguer, M.; Gouteron, J.; Jeannin, S.; Jeannin, Y.; Kahn, O. *Inorg. Chem*. **1984**, *23*, 4291.

(6) (a) Bürger, K.-S.; Chaudhuri, P.; Weighardt, K.; Nuber, B. *Chem. Eur. J*. **1995**, *1*, 583. (b) Chaudhuri, P.; Oder, K.; Wieghardt, K.; Gehring, S.; Haase, W.; Nuber, B.; Weiss, J. *J. Am. Chem. Soc*. **1988**, *110*, 3657.

(7) Xanthopoulos, C. E.; Sigalas, M. P.; Katsoulos, G. A.; Tsipis, C. A.; Terzis, A.; Mentzafos, M.; Hountas, A. *Inorg. Chem*. **1993**, *32*, 5433.

(8) Bakalbassis, E. G.; Bozopoulos, A. P.; Mrozinski, J.; Rentzeperis, P. J.; Tsipis, C. A. *Inorg. Chem*. **1988**, *27*, 529.

(9) Bakalbassis, E.; Bergerat, P.; Kahn, O.; Jeannin, S.; Jeannin, Y.; Dromzee, Y.; Guillot, M. *Inorg. Chem*. **1992**, *31*, 625.

(10) Hong, C. S.; Do, Y. *Inorg. Chem*. **1997**, *36*, 5684.

(11) Jotham, R. W.; Kettle, S. F. A.; Marks, J. A. *J. Chem. Soc., Dalton Trans*. **1972**, 428.

(12) Muto, Y.; Sasaki, A.; Tokii, T.; Nakashima, M. *Bull. Chem. Soc. Jpn*. **1985**, *58*, 2572.

(13) Harada, A.; Tsuchimoto, M.; Ohba, S.; Iwasawa, K.; Tokii, T. *Acta Crystallogr*. **1997**, *B53*, 654.

(14) Kato, M.; Muto, Y. *Coord. Chem. Rev*. **1988**, *92*, 45.

(15) Brandon, E. J.; Rittenberg, D. K.; Arif, A. M.; Miller, J. S. *Inorg. Chem.* **1998**, *37*, 3376.

(16) Drago, R. S. *Physical Methods for Chemists*, 2nd ed.; Saunders College Publishers: New York, 1992.

(17) A program for automatic solution and refinement of crystal structure. Altomare, A.; Burla, M. C.; Camalli, M.; Cascarano, G.; Giacovazzo, C.; Guagliardi, A.; Moliteni, A. G. G.; Polidori, G.; Spagna, R. (Release 1.02).

(18) Sheldrick, G. M. SHELX97. Programs for Crystal Structure Analysis (Release 97−2), University of Göttingen, Germany, 1977.

(19) Maslen, E. N.; Fox, A. G.; O'Keefe, M. A.; In *International Tables for Crystallography: Mathematical, Physical and Chemical Tables*, Wilson, A. J. C., Ed.; Kluwer: Dordrecht, The Netherlands, 1992; Vol. C, Chapter 6, p 476.

(20) Farrugia, L. J. *J. Appl. Crystallogr*. **1997**, *30*, 565.

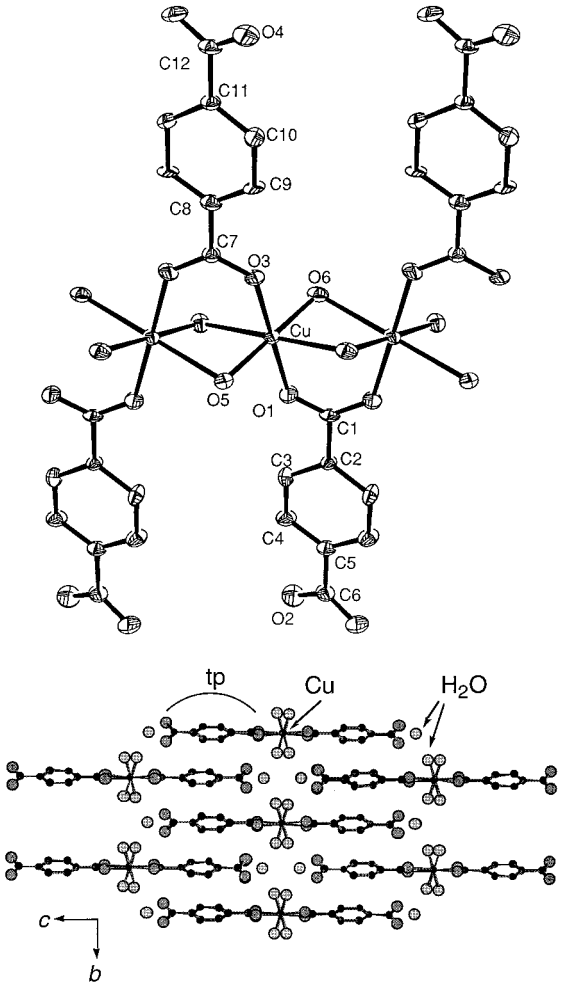

Figure 1. ORTEP (ellipsoids at 50% probability) view and numbering scheme for structure **1** (a, top) and packing arrangement perpendicular to chains along the crystallographic *b* and *c* axes (b, bottom).

romagnetic coupling ($J/k_B \approx -240$ K) between Cu(II) centers, and a spontaneous moment due to spin canting at 2.8 K. The large exchange coupling is attributed to the 2-D structure being comprised of a sheet of dimers, where the **tp** bridges include both bridging bidentate and monodentate binding modes. Generally, materials with only monodentate **tp**-bridged Cu(II) centers display weak antiferromagnetic coupling. Such interactions have been observed with tetracarboxylic acids linking Cu(II) metals to produce an extended 3-D structured material.[21] Recently, the formation of a bisbridging bidentate, 1,3,5-benzenetricarboxylato copper(II), structure has been reported, although the magnetic properties of this material were not investigated.[22]

The IR spectra of **1** and **2** exhibit very-strong-intensity bands in the 1200 and 1700 cm^{-1} regions. The bands for **1** at 1544 and 1398 cm^{-1} are assigned to the ν_{as}(COO) and ν_s(COO) stretching modes, respectively, of the bound bridging bismonodentate end of the **tp** ligand as shown in Figure 1. The 1428 cm^{-1} band is assigned to the ν_s(COO) stretching mode of the unbound portion of the **tp** ligand, with the ν_{as}(COO) mode overlapping that of the bound end of **tp**. The splitting between the bands of the bound bridging bis-monodentate end is $\Delta =$ 146 cm^{-1}, larger than that for the unbound end ($\Delta =$116 cm^{-1}). This is consistent with the larger carboxylate O−C−O bond angle of the **tp** ligand for the bound end as compared to the carboxylate end not bound to Cu(II).[23] The IR spectrum of **2** with ν_{as}(COO) and ν_s(COO) bands at 1579 and 1397 cm^{-1}, respectively, displays $\Delta = 182$ cm^{-1}, indicative of a monodentate binding mode where H-bonding occurs with the unbound CO group.[23]

Structure Description. 1 has the bridging bis-monodentate binding mode for **tp** (**C**) that leads to a 1-D chain structure, Figure 1a. The coordination geometry around the Cu(II) center is a tetragonally distorted octahedron with additional rhombic and trigonal distortions. Table 2 summarizes the key bond distances and angles for **1** and **2**. The average $Cu-O_{tp}$ bond distance is 1.923 Å, while the average $Cu-O_{H_2O}$ bond distance is 1.985 Å. The bond distances to the apical water molecules are 2.4771(26) and 2.4801(24) Å. Along the chain, the Cu centers are bridged by **tp** as well as by water molecules that occupy the axial positions on the neighboring Cu(II) complex. This results in the formation of asymmetrically bridged Cu(II) centers, as observed for acetate and water-bridged Cu(II) dimers.[24] The average angle at the bridging waters of 89.1 ± 0.2° leads to near parallel-planar Cu(II) complexes. The 1-D structure of **1** closely resembles that of the chains obtained from $Cu^{II}(O_2CPh)_2(H_2O)_3$.[25] The Cu···Cu distances in **1** are 3.150 Å along the chain, and 12.002 Å between chains. The torsion angle between the benzene plane and the carboxylato end group O1−C1−O1 plane is 13.2(3)°. Hydrogen bonding occurs between the 1-D chains, via the **tp** O atoms and the noncoordinated water molecules, increasing the structural dimensionality of this material, Figure 1b.

The basal plane with the Cu center of the distorted square-pyramidal Cu(II) complexes of **2** is shown in Figure 2a. These complexes are bridged via bound water at the apical position, forming a chain. These chains are then linked together through the bis-monodentate **tp** ligand (**B**), yielding a sheet structure, Figure 2b. The mirror plane present at the center of the **tp** ligand, through the C3 and C4 carbons, indicates that **tp** is *cis*-bound, via crystallographically equivalent oxygen atoms, O2. Typically, bis-monodentate (**B**) binding of **tp** produces *trans*-bound bridges.[5−8] The *cis*-conformation in **2** is likely stabilized by the hydrogen bonding present between the free CO group and the coordinated water of the neighboring complex along the chain. The Cu−O bond distance between the metal and the apical water is 2.424(4) Å, much longer than the other Cu−O bonds to **tp** (1.916(2) Å) or basal H_2O [1.944(3), 1.992(3) Å] ligands. The Cu−O−Cu bond angle is 117.88(15)°, leading to tilted basal planes as compared to the parallel-planar arrangement for **1**. The torsion angle between the benzene plane and the carboxylato end group O1−C1−O1 plane is 1.0(4)°. The Cu···Cu separation along the 1-D H_2O-bridged chain is 3.788 Å, while the long interchain **tp** bridges lead to a Cu···Cu distance of 10.743 Å. As with structure **1**, hydrogen bonding is present in **2** between coordinated water in the Cu basal plane (O4) and the free CO group of **tp**, leading to a 3-D extended structure.

Magnetic Properties. The 300 K axial X-band powder EPR spectra of **1** and **2** are typical of distorted Cu(II) complexes[26]

(21) Zou, J.-Z.; Liu, Q.; Xu, Z.; You, X.-Z.; Huang, X.-Y. *Polyhedron* **1998**, *17*, 1863.
(22) Chui, S. S.-Y.; Lo, S. M.-F.; Charmant, J. P. H.; Orpen, A. G.; Williams, I. D. *Science* **1999**, *283*, 1148.
(23) Deacon, G. B.; Phillips, R. J. *Coord. Chem. Rev.* **1980**, *33*, 227.
(24) Christou, G.; Perlepes, S. P.; Libby, E.; Folting, K.; Huffman, J. C.; Webb, R. J.; Hendrickson, D. N. *Inorg. Chem.* **1990**, *29*, 3657.
(25) Koizumi, H.; Osaki, K.; Watanabé, T. *J. Phys. Soc. Jpn.* **1963**, *18*, 117.
(26) Wilkinson, G., Gillard, R. D., McCleverty, J. A., Eds. *Comprehensive Coordination Chemistry*; Pergamon Press: Oxford, 1987; Vol. 5, p 594−767 and references therein.

Table 2. Selected Bond Lengths (Å) and Bond Angles[a](deg) for Cutp$(OH_2)_2$·H_2O (**1**) and Cu**tp**$(OH_2)_2$ (**2**)

Cu**tp**$(OH_2)_2$·H_2O (**1**)		Cu**tp**$(OH_2)_2$ (**2**)	
Cu−O3	1.9218(18)	Cu−O2	1.916(2)
Cu−O1	1.9236(18)	Cu−O2^{v}	1.916(2)
Cu−O5(W)	1.988(3)	Cu−O3(W)	1.992(3)
Cu−O6(W)	1.979(3)	Cu−O3(W)^{iv}	2.424(4)
Cu−O5(W)^{ii}	2.4801(24)	Cu−O4	1.944(3)
Cu−O6(W)^{i}	2.4771(26)	O2^{iv}−Cu−O2	178.0(4)
O3−Cu−O1	179.49(17)	O2−Cu−O4(W)	90.47(7)
O3−Cu−O6(W)	89.57(13)	O2−Cu−O3(W)	89.51(7)
O1−Cu−O6(W)	90.24(14)	O4(W)−Cu−O3(W)	178.64(19)
O3−Cu−O5(W)	90.44(14)	O2−Cu−O3(W)^{iv}	90.9(2)
O1−Cu−O5(W)	89.74(14)	O4(W)−Cu−O3(W)^{iv}	90.19(16)
O6(W)−Cu−O5(W)	179.70(15)	O3(W)−Cu−O3(W)^{iv}	91.17(10)
C1−O1−Cu	129.8(2)	Cu−O3(W)−Cu^{vi}	117.78(15)
C7−O3−Cu	130.1(2)	C1−O2−Cu	116.4(4)
Cu−O5(W)−Cu^{ii}	88.92(10)		
Cu−O6(W)−Cu^{i}	89.33(10)		
torsion angle between the benzene plane and COO end-group	13.2(3)		1.0(4)
dihedral angle between basal plane and O−C−O plane	117.27−117.44		2.3−5.5

[a] Standard deviations of the last significant figures are given in parentheses. Symmetry codes: (i) $-x+1, -y, z$; (ii) $-x, -y, z$; (iii) $-x-1, y, z$; (iv) $-x, -y+1, z-1/2$; (v) $-x, y, z$; (vi) $-x, -y+1, z+1/2$.

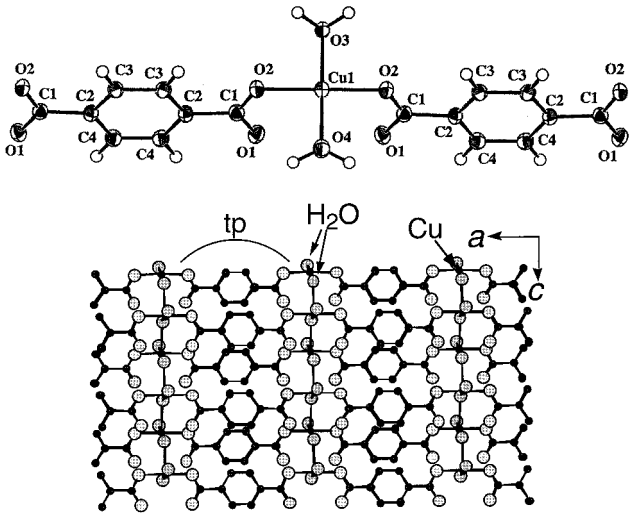

Figure 2. ORTEP (ellipsoids at 50% probability) view and numbering scheme for structure **2**a, top and view of the 2-D sheet structure along the crystallographic *a* and *c* axes (b, bottom).

with $g_\perp = 2.08$, $g_\parallel = 2.29$ (**1**) and $g_\perp = 2.07$, $g_\parallel = 2.29$ (**2**). Hence, $\langle g \rangle = 2.15$ and 2.14 for **1** and **2**, respectively. The spectra do not show signs of exchange interaction at 300 K. As $g_\parallel > g_\perp$, this suggests that the unpaired electron resides in a $d_{x^2-y^2}$ orbital, expected for tetragonally elongated octahedral and square-pyramidal complex geometries.

The magnetic susceptibilities, χ, of **1** and **2** were measured between 2 and 300 K at 5 kG, and Figures 3 and 5 show the plots of χT and χ^{-1} vs T. Above 50 K the data for **1** can be fit to Curie−Weiss law with $\theta = -7.2$ K, indicating antiferromagnetic coupling. The room-temperature effective moment, μ_{eff} [$\equiv(8\chi T)^{1/2}$], is 1.80 μ_B, in good agreement with the expected value of 1.86 μ_B assuming $g = 2.15$. The $\chi T(T)$ data are nearly constant to ~100 K and then drop rapidly and approach zero at low temperature, Figure 3a. Over the entire temperature range the data are best fit by the Bonner−Fisher model for a uniformly spaced chain of $S = 1/2$ metal centers,[27] using $\mathbf{H} = -2J\mathbf{S}_1\cdot\mathbf{S}_2$ and the numerical expression[28]

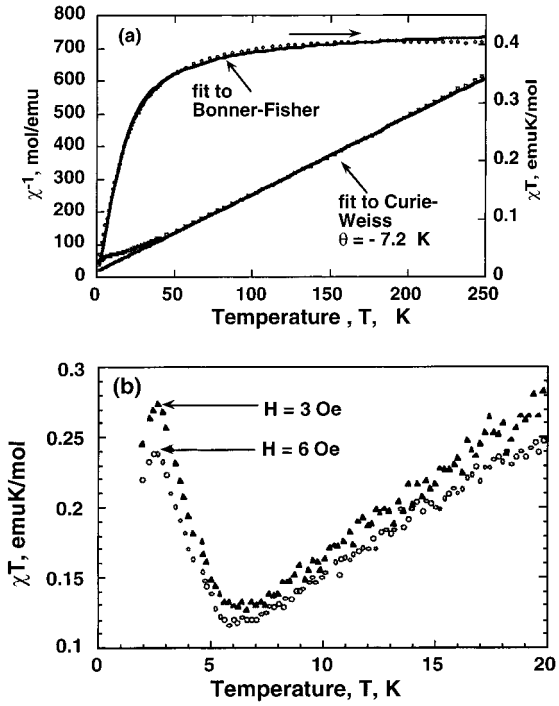

Figure 3. Magnetic susceptibility of **1** as (a) $\chi T(T)$ and $\chi^{-1}(T)$ at $\mathbf{H} = 0.5$ T with the $\chi^{-1}(T)$ fit to the Curie−Weiss law and the $\chi T(T)$ fit to the Bonner−Fisher expansion with $\langle g \rangle = 2.15$, and (b) $\chi T(T)$ at $\mathbf{H} = 3$ and 6 Oe.

$$\chi = \frac{Ng^2\beta^2}{kT}\,\frac{0.25 + 0.074975x + 0.075235x^2}{1.0 + 0.9931x + 0.172135x^2 + 0.757825x^3} \quad (1)$$

where

$$x = |J|/kT \quad (2)$$

with $\langle g \rangle = 2.15$ as determined from the powder EPR spectrum. This fit yields an exchange coupling constant of J/k_B of −9.15 K. This value is similar to that obtained for Cu(benzoate)$_2$(H_2O)$_3$

(27) Bonner, J. C.; Fisher, M. E. *Phys. Rev.* **1964**, *A135*, 640.

(28) Estes, W. E.; Gavel, D. P.; Hatfield, W. E.; Hodgson, D. *Inorg. Chem.* **1978**, *17*, 1415.

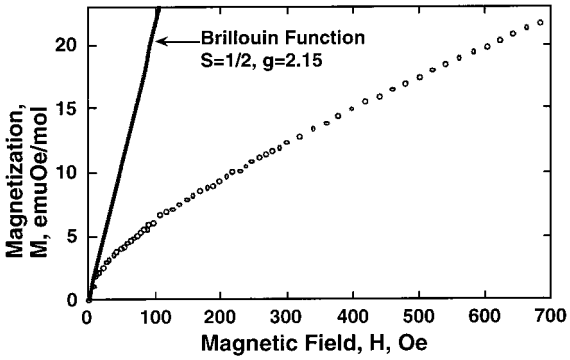

Figure 4. Magnetization of **1** to 700 Oe at 2 K with a plot of the Brillouin function for $S = 1/2$ at 2 K with $g = 2.15$.

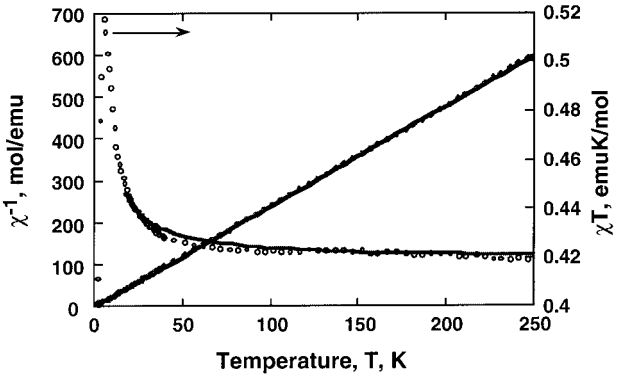

Figure 5. Magnetic susceptibility of **2** as $\chi T(T)$ between 2 and 300 K at $\mathbf{H} = 0.5$ T with a fit to the Baker expansion ($\langle g \rangle = 2.14$) with molecular field correction ($z = 2$) between 30 and 300 K and as $\chi^{-1}(T)$ with a Curie−Weiss fit ($\theta = -0.8$ K) between 80 and 300 K.

chain structured material for which $J/k_B = -9.1$ K.[29] Thus, magnetically, **1** behaves as a 1-D chain with appreciable antiferromagnetic interactions between the $S = 1/2$ Cu(II) sites.

In a small applied field ($H \leq 10$ Oe) $\chi T(T)$ reaches a minimum 6.5 K before increasing to a maximum at 2.5 K, Figure 3b. This is attributed to the onset of a spontaneous moment. This onset was confirmed by 10 Hz $\chi'(T)$ and $\chi''(T)$ data, which increase with decreasing temperature; however, no maxima were observed, indicating that long-range magnetic ordering was not achieved.

The field dependence of the magnetization, $M(H)$, at 2 K, Figure 4, displays a sharp increase in magnetization below 20 Oe, followed by a leveling off of the magnetization at higher fields. The magnetization does not saturate at 5 T, but reaches a value of 616 emu Oe/mol, indicative of antiferromagnetically coupled spins. The data are substantially less than those expected for an independent spin as calculated using the Brillouin function, Figure 4. The observation of a spontaneous moment is consistent with the presence of canted spins, and has been reported to occur for $Cu(benzoate)_2(H_2O)_3$.[29]

The superexchange pathway by which the Cu(II) atoms are antiferromagnetically coupled is the bridging **tp** ligand. Although the dominant antiferromagnetic interaction in **1** occurs via the **tp** bridge, there exists an additional superexchange pathway. Each Cu(II) is also bridged by two water molecules. The study of the magnetic properties of chloro-bridged parallel-planar Cu(II) complexes indicates that the bridge angle is the most important factor in determining the sign of the exchange coupling constant. The bridge angles at the bridging water between the Cu centers in **1** are 88.92(10) and 89.33(10)°. Such bond angles in parallel-planar chloro-bridged dimers have been reported to display both weak ferro- and antiferromagnetic interactions.[30] As the CuO_{H_2O} bond length is long, 2.48 Å, any interaction along this superexchange pathway would likely be very weak. Therefore, the overall interaction observed along the chain for **1** is dominated by the magnetic interaction, via the **tp** bridge.

In contrast to **1**, the $\chi^{-1}(T)$ ($T > 60$ K) data for **2** can be fit to the Curie−Weiss expression with $\theta = 0.8$ K, suggestive of weak ferromagnetic coupling, Figure 5. The room temperature μ_{eff} is 1.83 μ_B, in good agreement with the expected value of 1.85 μ_B assuming $g = 2.14$. $\chi T(T)$ was also fit above 50 K to the Baker equation,[31] eqs 3−6 applicable for chains of $S = 1/2$

$$\chi = \frac{Ng^2\beta^2}{4kT}\left[\frac{N}{D}\right]^{2/3} \tag{3}$$

$$N = 1.0 + 5.7979916y + 16.902653y^2 + 29.376885y^3 + 29.832959y^4 + 14.036918y^5 \tag{4}$$

$$D = 1.0 + 2.7979916y + 7.0086780y^2 + 8.653644y^3 + 4.5743114y^4 \tag{5}$$

$$y = J/2kT \tag{6}$$

metal centers, which, using $\langle g \rangle = 2.14$, resulted in a J/k_B value of +0.6 K. Here, the interaction between the Cu(II) metal centers along the chain via the bridging water molecule involves weak ferromagnetic coupling. The Baker expression displays a more rapid increase in $\chi T(T)$ with decreasing temperature ($T < 70$ K) than that observed for **2**. A molecular field correction[32] using

$$\chi_{2-D} = \frac{\chi_{1-D}}{[1 - \chi_{1-D}(2zJ'/Ng^2\beta^2)]} \tag{7}$$

where z is the number of interacting neighbors (i.e., 2), was applied to $\chi T(T)$ above 30 K, yielding a J'/k value of −0.13 K.[33] This correction accounts for magnetic interactions not occurring along the chain, but in the second dimension via the **tp**. Differences between the fit and data around 50 K are attributed to additional magnetic interactions occurring due to hydrogen bonding to the CO group. In contrast to **1**, **2** does not display the $M(H)$ of **1**, but fits the Brillouin function with $\theta = 0.8$ K at 5 K to account for the weak ferromagnetic interactions, Figure 6. At 2 K, however, the $M(H)$ is significantly lower than that for the Brillouin at this temperature with $\theta = 0.8$ K, indicating that, at this temperature, antiferromagnetic interactions are now dominate. The lack of maxima in the $\chi'(T)$ and $\chi''(T)$ are also consistent with the lack of long-range magnetic ordering.

These results indicate an antiferromagnetic interaction occurring between chains via the **tp** bridges. The magnitude and sign of the exchange coupling constant obtained from the fit are similar to those observed for weakly coupled bis-monodentate **tp**-bridged Cu(II) dimers.[5,7] In **2** the coplanarity required

(29) Dender, D. C.; Davidovic, D.; Reich, D. H.; Broholm, C.; Lefmann, K.; Aeppli, G. *Phys. Rev. B* **1996**, *53*, 2583.
(30) Marsh, W. E.; Hatfield, W. E.; Hodgson, D. J. *Inorg. Chem.* **1982**, *21*, 2679 and references therein.
(31) Baker, G. A.; Rushbrooke, G. S., Jr.; Gilbert, H. E. *Phys. Rev.* **1964**, *135*, A1272.
(32) Myers, B. E.; Berger, L.; Friedberg, S. A. *J. Appl. Phys.* **1968**, *40*, 1149.
(33) Analysis of χT using Curie−Weiss ($\theta = 0.8$ K) did not yield an improved fit to the data.

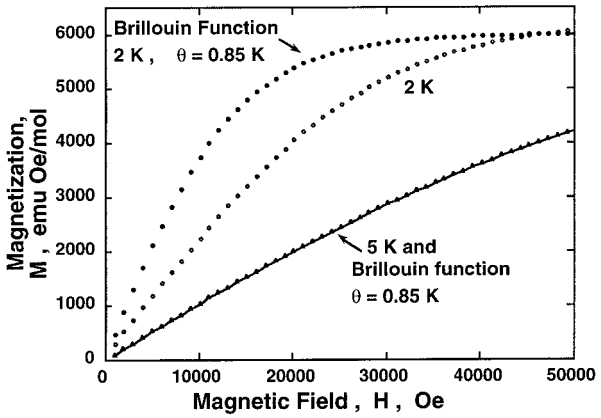

Figure 6. Magnetization of **2** as a function of the field at 2 and 5 K, with the 5 K plot fit to the Brillouin function ($\langle g \rangle = 2.14$) with $\theta =$ 0.8 K.

for strong antiferromagnetic interactions is not obtained as the dihedral angle between Cu-containing basal planes is 2.3−5.5°, the dihedral angle between the Cu basal plane and the carboxylato end is 12°, and the torsion angle between the carboxylato end and benzene ring is 1°.

The superexchange pathway in **2** that leads to the ferromagnetic interactions in the 1-D chain is attributed to the bridging apical water bridge as there is no short **tp** bridge as in **1**. The bridging angle is 117.78(15)°, larger than that observed for **1**. Generally, in the case of chloro-bridged parallel-planar Cu(II) complexes, bridge angles significantly larger than 90° lead to antiferromagnetic coupling between metal centers.[30] The weak ferromagnetic behavior of **2** along this water bridge is attributed to the favorable orbital orientations at the water oxygen atom that allows only for interaction between the $d_{x^2-y^2}$ orbital of the upper complex and the d_{z^2} orbital of the lower complex. Here, only one Cu(II) complex interacts with the bridge via a magnetic orbital ($d_{x^2-y^2}$), as d_{z^2} does not contain the lone spin. A systematic study of the magnetic properties of water-bridged parallel-planar complexes as a function of bridge angle and bond distances has not been reported.

The thermogravimetric analyses of **1** and **2** after magnetic measurements confirm that neither sample lost coordinated water molecules. The heating of **1** and **2** leads to a weight loss of 15% and 12%, respectively, corresponding to the loss of two water molecules (∼14%). Note that **1** does undergo dehydration, losing the noncoordinated water molecule. Above 300 °C, both samples undergo decomposition as seen from the emergence of CO_2 peaks in the mass spectrum. The integrity of the samples during magnetic measurements supports the above description of the superexchange pathway occurring via coordinated water molecules.

Acknowledgment. We are grateful for funding provided by the U.S. Department of Energy (DOE) (Grant No. DEFG 03-93ER45504). L.D. is thankful for a postdoctoral fellowship provided by Fonds FCAR, Québec.

Supporting Information Available: This material is available free of charge via the Internet at http://pubs.acs.org. X-ray crystallographic files for both **1** and **2**, in CIF format.

IC990400R